INTERFACE

royalsocietypublishing.org/journal/rsif

Research

Cite this article: Li X, Thirumalai D. 2019 Share, but unequally: a plausible mechanism for emergence and maintenance of intratumour heterogeneity. *J. R. Soc. Interface* **16**: 20180820.
http://dx.doi.org/10.1098/rsif.2018.0820

Received: 1 November 2018
Accepted: 30 November 2018

Subject Category:
Life Sciences–Physics interface

Subject Areas:
biophysics, computational biology, evolution

Keywords:
intratumour heterogeneity, evolution, public goods, allocation strategy, cooperation, competition

Authors for correspondence:
Xin Li
e-mail: xinlee0@gmail.com
D. Thirumalai
e-mail: dave.thirumalai@gmail.com

Electronic supplementary material is available online at https://dx.doi.org/10.6084/m9.figshare.c.4329443.

THE ROYAL SOCIETY PUBLISHING

Share, but unequally: a plausible mechanism for emergence and maintenance of intratumour heterogeneity

Xin Li and D. Thirumalai

Department of Chemistry, University of Texas at Austin, Austin, TX 78712, USA

XL, 0000-0002-2510-2236; DT, 0000-0003-1801-5924

Intratumour heterogeneity (ITH), referring to the coexistence of different cell subpopulations in a single tumour, has been a major puzzle in cancer research for almost half a century. The lack of understanding of the underlying mechanism of ITH hinders progress in developing effective therapies for cancers. Based on the findings in a recent quantitative experiment on pancreatic cancer, we developed a general evolutionary model for one type of cancer, accounting for interactions between different cell populations through paracrine or juxtacrine factors. We show that the emergence of a stable heterogeneous state in a tumour requires an unequal allocation of paracrine growth factors (public goods) between cells that produce them and those that merely consume them. Our model provides a quantitative explanation of recent *in vitro* experimental studies in pancreatic cancer in which insulin-like growth factor II (IGF-II) plays the role of public goods. The calculated phase diagrams as a function of exogenous resources and fraction of growth factor producing cells show ITH persists only in a narrow range of concentration of exogenous IGF-II. Remarkably, maintenance of ITH requires cooperation among tumour cell subpopulations in harsh conditions, specified by lack of exogenous IGF-II, whereas surplus exogenous IGF-II elicits competition. Our theory also quantitatively accounts for measured *in vivo* tumour growth in glioblastoma multiforme (GBM). The predictions for GBM tumour growth as a function of the fraction of tumour cells are amenable to experimental tests. The mechanism for ITH also provides hints for devising efficacious therapies.

1. Introduction

Cancer, a complex disease that arises through clonal evolution, is a major cause of mortality throughout the world with no cure in sight despite a tremendous amount of effort and resources expended to uncover its root causes. The underlying mechanisms of the origin and spread of cancer is still under debate [1]. The first evolutionary theory of cancer, proposed by Nowell in 1976, describes cancer progression as a linear process derived from sequential acquisition of somatic mutations [2]. With the advent of next-generation sequencing [3], it has become clear that instead of linear growth, cancer evolution is better described by branched growth in which multiple subclones appear and coexist during cancer progression. Accumulating evidence favours the branched model and the associated intratumour heterogeneity (ITH) [4–11]. ITH is a complex phenomenon and many sources, such as genetic, epigenetic mutations, stochastic genetic expression and so on, could contribute to its origin [12]. The presence of ITH in a variety of cancers, which is a great impediment to designing effective treatments [12–14], is hard to rationalize according to the linear evolutionary model because subclones with even a small fitness advantage should ultimately proliferate at the expenses of others. For this reason, the persistence of ITH in a macroscopic tumour is a puzzle.

The tumour cells, with diverse genetic or epigenetic mutations, are often spatially separated [4,7] with each subclone dominating the cell population in a specific region. It indicates that spatial constraints or distinct microenvironments might prohibit clonal sweeps, thus inducing ITH. However, it cannot explain the coexistence of distinct subclones in the same region of a tumour [15,16].

The interactions between tumour cells and the surrounding normal cells, and microenvironments have been extensively studied in the past few decades [17–20] while much less effort has been made in investigating the interactions among subclonal populations in tumours. Instead of competition, the cooperation among distinct subclonal populations is found to be essential for tumour maintenance [21], enhance tumour growth [22] and even facilitate cancer metastasis [23,24]. Meanwhile, it is observed that a minor and even undetectable subclone can dominate the clinical course and lead to cancer relapse frequently [25–27]. Therefore, it is crucial to understand the mechanism of cooperation that facilitates the emergence and maintenance of ITH in a single tumour.

Cooperation can be established through mutualism or even unidirectional interactions among different subpopulations. Mutualism in ecology provides an effective mechanism for the establishment of a heterogeneous state in which each subpopulation benefits from the activity of the other [28–31]. Recently, it was found that two distinct subclones in cancer can complement each other's deficiency in order to survive and proliferate [21]. The formation of a heterogeneous state can be explained by a mechanism similar to mutualism in which fitness of distinct cell types is maximized by resource sharing [32]. Compared to the strict interdependence in mutualism, a unidirectional interaction between distinct populations is observed more frequently [32–34]. It is quite common to find that some tumour cells secrete diffusible growth factors or other paracrine factors to promote tumour growth [32]. Meanwhile, other types of tumour cells free ride on those essential nutrients to grow and might even dominate the whole population without producing them. One recent study for glioblastoma multiforme (GBM) shows that a minor subclone in a tumour supports and promotes the growth of a dominant one by activating a paracrine signalling circuit [34]. It was found that the mixture of these two distinct subpopulations promote faster tumour growth than they would by themselves. Similarly, an insightful *in vitro* experiment combined with theoretical analysis based on evolutionary game theory [35] investigated the 'public goods' game in pancreatic cancer cell populations in which one cell type produces a growth factor as the 'public good'. The growth factors promote the proliferation of both cell types. It is found that these two types of cancer cells can coexist under certain conditions although there is only a unidirectional interaction between them. Although insightful, previous applications of the evolutionary game theory provided only a qualitative explanation for the experimental results [35]. The assumption that the population size is a constant does not accurately capture the growth dynamics observed in their experiments. In addition, as shown here, such an assumption cannot account for the intriguing related phenomena of glioblastoma multiform growth [34] in which there are clear manifestations of ITH. Additionally, a theoretical framework accounting for influences of different factors such as exogenous resources and the cost for producing public goods on the establishment of cooperation between two cell populations directly is needed for expanding the scope of the game theory applications. Therefore, the underlying generality of the mechanisms for the origin of ITH is still unclear.

Here, we investigate the mechanism of cooperation between two distinct populations composed of 'producers' and 'non-producers'. We show that several factors are indispensable for the maintenance of a stable heterogeneous coexisting population of producer and non-producer cells. A critical finding in our work is that the unequal allocation of public goods among different species plays a crucial role in maintaining heterogeneity. By studying the influence of exogenous resources and initial population fraction on such a simple system, we obtained a phase diagram from our theory, which is in excellent agreement with experimental observations. Our theory also quantitatively explains the unexpected growth behaviours of GBM tumours as a function of initial fractions of producer cells in *in vivo* experiments with no free parameters. The robustness of the theory is established by making testable predictions of the origin of ITH in GBM driven by a paracrine mechanism [34]. The discovery of mechanisms for such ITH might also give clues for changing strategy of treatment in cancers in which interactions between different subclones are prevalent.

2. Models

The public goods game has been extensively used in the studies of human societies, and similar concepts have been applied to other systems, such as microbial colonies and insect communities [36–41]. In this model, both the producer and non-producer benefit from the products produced solely by the former (figure 1). However, the producers pay a price for the production of public goods while the non-producers merely free-ride on the products without incurring any cost. In general, such a dynamic would result in an unstable system in the sense that the producer might become extinct if the public goods are shared equally between the parties. The system would collapse unless sufficient exogenous resources are provided, which could lead to the fixation of non-producers, as discussed below in detail.

2.1. Equal sharing is untenable

We describe the evolution of the fraction f_+ of producers and f_- of non-producers using the replicator equations

$$\frac{\partial f_+}{\partial t} = (w_+ - \langle w \rangle) f_+ \tag{2.1}$$

and

$$\frac{\partial f_-}{\partial t} = (w_- - \langle w \rangle) f_-, \tag{2.2}$$

where w_+ and w_- are fitness of producers and non-producers, respectively. The normalization condition is $f_+ + f_- = 1$. The average fitness $\langle w \rangle$ is

$$\langle w \rangle = w_+ f_+ + w_- f_-. \tag{2.3}$$

Let N_+ and N_- be the number of producers and non-producers, respectively. The total population size is $N \equiv N_+ + N_-$. Although the system size, N, is often assumed to be a constant [35,42], we consider a general case [43] where the population size varies with the time evolution given by

$$\frac{\partial N}{\partial t} = w_+ N_+ + w_- N_- = \langle w \rangle N. \tag{2.4}$$

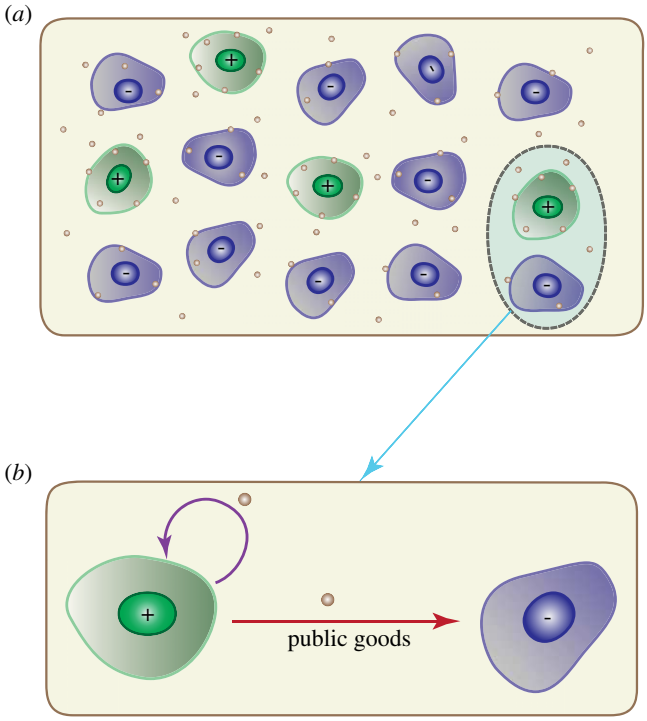

Figure 1. Illustration of the public goods game. (*a*) The public goods (small brown circles) generated by producers ('+' agents in green) are shared unequally between producers and non-producers ('−' agents in blue colour). Both producers and non-producers benefit from the presence of the public goods, which promote proliferation or survival of these agents. The public goods can also be supplied from exogenous resources. (*b*) A zoom-in of the dashed line oval in figure 1*a* to illustrate the public goods dependent circuit for the producer and non-producer. Coexistence of the two cell types requires feedback (purple line) and unequal sharing of the public goods.

Agent death, neglected for simplicity, could be readily included in the fitness functions.

If the public goods are shared among all the producers and non-producers equally, the same benefit will be presented to them, leading to the relation

$$w_+ = w_- - p_0, \tag{2.5}$$

where p_0 (>0) is the cost paid by the producers to generate the public goods. Then, the time evolution of producers could be rewritten as

$$\frac{\partial f_+}{\partial t} = -p_0 f_+(1 - f_+). \tag{2.6}$$

Therefore, the fraction of producers would decrease with time until it vanishes because p_0, f_+, and $1 - f_+$ are all non-negative. Then, the non-producers could sweep through the population, achieving higher fitness in the process, if exogenous public goods are provided continuously to support the population growth. Otherwise, the system would collapse as observed in the case of 'tragedy of the commons' once the public goods are depleted [44].

3. Results

3.1. Coexistence between producers and non-producers requires nonlinear fitness

A solution to the dilemma that emerges from the naive model of equal sharing, discussed above, is to change the rule for the allocation of public goods. Because the producer pays a price for the production of public goods, which decreases its fitness directly, more products should be allocated to the producer (see the public goods distribution in figure 1*a* as an example). If this were to occur, the producer would recoup the losses in order to gain the same fitness as the non-producer. In this unequal sharing scenario, the producer and non-producer could coexist, as we show here.

In general, the fitness of one agent is a function of the fraction of producers. A higher fitness is expected as the fraction of producers increases. For a dynamic system, a heterogeneous state (containing both producers and non-producers) could be maintained only the stabilities of the states are ensured. A heterogeneous state cannot be realized if w_+ and w_- are linear fitness functions of f_+. Let the fitness functions of the producer (w_+) and non-producer (w_-) be

$$w_+ = k_+ f_+ - p_0 \tag{3.1}$$

and

$$w_- = k_- f_+, \tag{3.2}$$

respectively. The parameters k_+, k_- are the corresponding allocation coefficients of public goods produced by producers and p_0 is the cost paid by each producer. The producer needs to get more public goods than the non-producer, which means $k_+ > k_-$ ($k_+ = k_-$ in equation (2.5)). The condition for equilibrium with both players follows from equations (2.1) and (2.2), resulting in

$$f_+^0 = \frac{p_0}{k_+ - k_-}. \tag{3.3}$$

Given the fraction f_+^0 for the producer in equation (3.3), the two members attain the same fitness ($w_+ = w_-$). However, this equilibrium is unstable and eventually only one of them survives (see electronic supplementary material, figure S1). As the fraction f_+ becomes a little higher than f_+^0 due to the birth of new producers or a higher value is given initially, the producer would attain higher fitness than the non-producer (for $k_+ > k_-$), leading to a much higher fraction of the producer. Finally, the producer would take over the whole population due to this positive feedback. In the opposite limit, the system would consist of non-producer only if f_+ is smaller than f_+^0. Therefore, a linear fitness function cannot lead to the establishment of a stable heterogeneous system in the present model. Instead of a linear function, fitness functions are typically nonlinear in biological systems at all length scales due to cooperation or competition between the various interacting moieties [45–48]. In the following, we first use data from one recent experiment to illustrate how a stable heterogeneous population can be established from the public goods game in a system consisting of both producers and non-producers where a nonlinear relation is observed for fitness functions [35].

In a recent study, Archetti, Ferraro and Christofori (AFC) investigated the origin of the 'tragedy of the commons' in cancer cells [35]. The insulin-like growth factor II (IGF-II) is up-regulated in many cancers, which can promote cell proliferation and abrogate apoptosis [49,50]. The producer (+/+) cells are derived from mice with insulinomas (a neuroendocrine pancreatic cancer), while the non-producer (−/−) cells are obtained from the same mice but with IGF-II gene deleted. Therefore, the −/− cells do not produce the IGF-II molecules. Thus, IGF-II is an ideal public good for these two cell types

because both of them can uptake this protein to reach higher fitness (growth rate), ensuring their survival and growth. The two different types of cells were then mixed to investigate the conditions under which a stable heterogeneous state could be established, mediated by optimal sharing of IGF-II. Although AFC proposed a sound analyses of their findings based on game theory, only qualitative comparisons to their experiments were provided. In addition, the assumption of a constant population size [51] also requires scrutiny. Here, we approach the problem from a different perspective relying on the replicator dynamics with evolving population size, which enables us to make quantitative predictions not only for pancreatic cancer but also GBM.

The measured growth rate of the non-producer $-/-$ cells as a function of exogenous IGF-II concentration, c, is nonlinear (see electronic supplementary material, figure S2). In order to solve the replicator equations, we first fit the experimentally measured $-/-$ cell growth rate using a Hill-like function

$$w_- = a_1 + \frac{\lambda_1 c^\alpha}{a_2^\alpha + c^\alpha}. \tag{3.4}$$

The Hill function in equation (3.4) fits the experimental data accurately (see electronic supplementary material, figure S2) yielding $a_1 = 2.0$, $\lambda_1 = 18.9$, $\alpha = 0.7$ and $a_2 = 3.2$. We also used the logistic function, which does not fit the data nearly as well, to make predictions (see electronic supplementary material, figures S3 and S4 for details). Interestingly, the use of logistic function for the fitness yields qualitatively similar results (see electronic supplementary material, figures S3 and S4 for details), thus demonstrating that nonlinear feedback between $+/+$ and $-/-$ cells is the source of heterogeneity, as already surmised by AFC. We describe the results in the rest of the paper using the Hill-like function for w_+ and w_-.

The public good IGF-II is produced endogenously or can be supplied exogenously. Therefore, we write the IGF-II (c_-) available for the non-producer as

$$c_- \equiv c = bf_+ + c_0. \tag{3.5}$$

where c_0 represents the exogenous supply of IGF-II, and $b f_+$ is the allocation of IGF-II arising from $+/+$ cells. Because AFC did not measure the fitness of the producer cells systematically, a relation similar to that in equation (3.4) for w_+, might be assumed. In order for the emergence of heterogeneous populations, the allocation of public goods produced by the $+/+$ cells should be unequal, so the growth rate of $+/+$ cells is written as

$$w_+ = g(c_+) - p_0, \tag{3.6}$$

where $g(c_+)$ has the same Hill-like functional form as in equation (3.4) except that c is replaced by c_+, leading to

$$c_+ = af_+ + c_0. \tag{3.7}$$

The parameter a, similar to b in equation (3.5), is the coefficient for the allocation of IGF-II produced by $+/+$ cells.

3.2. Influence of public goods allocation strategies

First, let us consider the influence of allocation strategies for public goods in a mixture of $+/+$ and $-/-$ cells. The ratio of b/a in equations (3.5) and (3.7) determine how the public goods provided by the producers are shared between the two populations. The public goods are shared equally if the ratio (b/a) is equal to unity, while the producers do not provide resources to the non-producer if $b/a = 0$. More resources are allocated to the producer if $b/a < 1$ while the non-producer obtains a larger amount of resources as $b/a > 1$. Public goods (IGF-II) is diffusible, which is modelled in our theory in the following way. The equality ($a = b$) would result if diffusion of IGF-II is rapid. On the other hand, the inequality, $a > b$, would be a consequence of slow diffusion or fast uptake of IGF-II by the producers. The assumption of slow diffusion, with a limited diffusion range of IGF-II, is made in the model of AFC [35]. Thus, by considering different values of the ratio, b/a, different rates of diffusion and uptake of IGF-II are covered. Accordingly, three values 1, 0 and 0.1 are considered for the ratio b/a in figure 2*a–c*, which show the growth rate of the two cell types as a function of the fraction (f_+) of $+/+$ cells. The corresponding evolution of $f_+(t)$ under different initial conditions are also shown in figure 2*d–f* .

The $-/-$ cells always grow faster than $+/+$ cells if the public goods are shared equally ($b/a = 1$) (figure 2*a*), which can also be derived from equations (3.4) and (3.6) directly ($w_- > w_+$ for $b \geq a$). The non-producer always attains higher fitness than the producer as long as the former gets a larger ($b/a > 1$) or equal ($b/a = 1$) amount of IGF-II. Therefore, the non-producer would take over the whole population if $b/a \geq 1$ producing a homogeneous state, irrespective of the initial fraction $f_+(0)$ of the producer (see the evolution of $f_+(t)$ in figure 2*d*). The exception is when $f_+(0) = 1$. The state with producers only ($f_+ = 1$, see the open circle in figure 2*a*) is unstable under infinitesimal perturbations of non-producer population. A steady binary system with the coexisting population of $+/+$ and $-/-$ cells cannot form under these conditions, as expected from previous arguments.

Consider another limiting case with $b/a = 0$ in which the non-producer does not get access to the public goods generated by the producer (with $w_- = $ const., see the dash-dotted blue line in figure 2*b*). In this limit, it is possible to have an internal equilibrium (see the open circle in figure 2*b*) resulting in the two cells having the same fitness ($w_- = w_+$). However, this is an unstable equilibrium state, which means only one type of population would survive (see the filled red and blue circles in figure 2*b*, respectively) depending on the initial conditions (see also the evolution of $f_+(t)$ in figure 2*e*). A stable homogeneous state consisting of only producers results if $f_+(0)$ is above the fraction (f_+^{us}) of the producer corresponding to the internal unstable state (illustrated by the open circle in figure 2*b*). In this case, the flow is towards the $f_+(0) = 1$ stable state. For $f < f_+^{\mathrm{us}}$, the non-producers form another stable homogeneous state (see the green dotted and blue dash-dotted lines in figure 2*e*). A stable heterogeneous state with coexisting populations cannot exist if $b/a = 0$.

If the public goods are allocated unequally between the $+/+$ and $-/-$ cells due to the presence of spatial structure, (figure 2*c*) with $0 < b/a < 1$, two internal equilibrium states (with $0 < f_+^i < 1$) appear. One of them is an unstable state (the left open circle in figure 2*c*), whereas the filled green circle in figure 2*c* corresponds to a stable state due to the frequency-dependent selection [35,52]. Close to the internal stable state, the fitness of $+/+$ cells becomes smaller than that of $-/-$ cells as the $+/+$ cell frequency increases above the stable state value. Therefore, the frequency of $+/+$ ($-/-$) cells will decrease (increase) until it returns to the value corresponding to the stable state (see the yellow

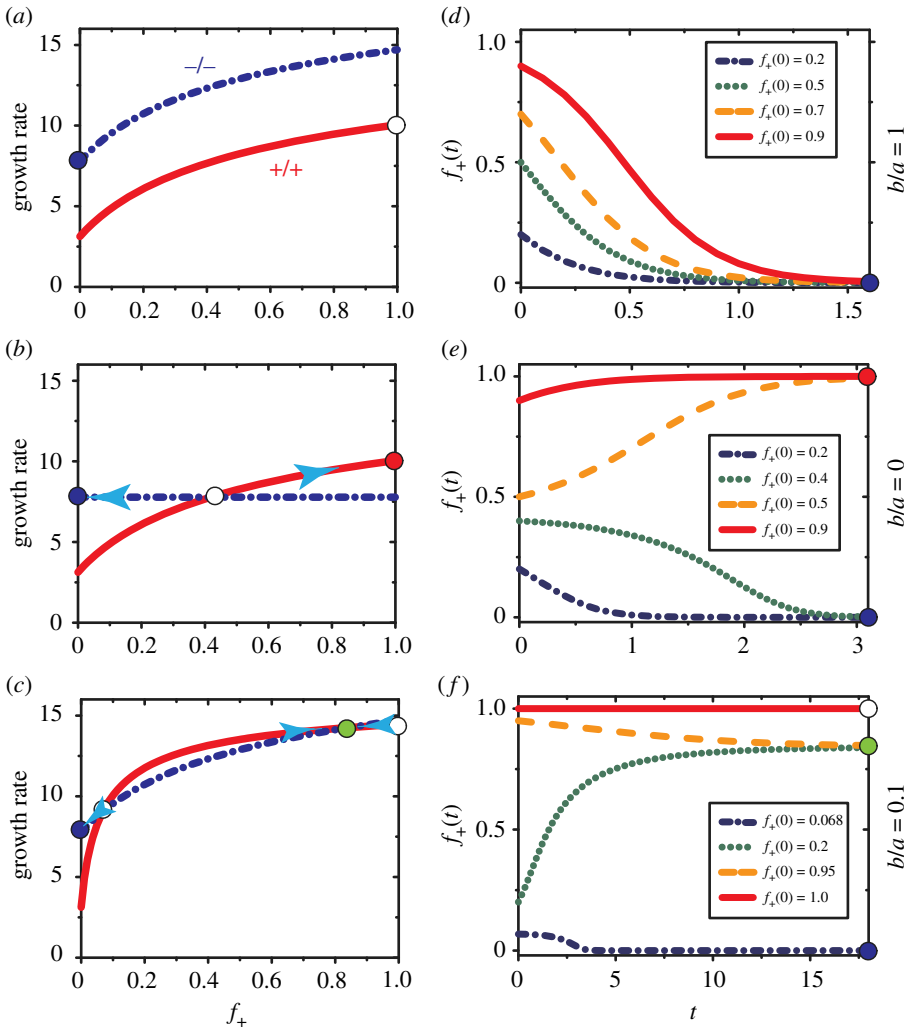

Figure 2. (*a*)–(*c*) Growth rates of $+/+$ and $-/-$ cells as a function of the fraction (f_+) of $+/+$ cells under different allocation of IGF-II produced by the $+/+$ cells. (*a*) Equal share of IGF-II ($b = a = 8$), (*b*) no share ($b = 0$ and $a = 8$), (*c*) a small portion ($b = 8$ and $a = 80$) is allocated to $-/-$ cells. The value of $c_0 = 1$ and $p_0 = 4.65$ in equation (3.6) are derived from fitting the equilibrium fractions of $+/+$ cells observed in experiments using our model. The growth rate of $+/+$ cells are shown in solid red lines while dash-dotted blue lines describe the growth rate of $-/-$ cells. The filled and empty circles indicate a stable or unstable fixed point, respectively. A stable state consisting of only $+/+(-/-)$ cells is indicated in red (blue) colour. The filled green circle shows a stable heterogeneous state representing coexistence of the two cell types. (*d*–*f*): The evolution of $f_+(t)$ at different $f_+(t = 0)$ values corresponding to the allocation strategies of IGF-II in (*a*–*c*). Each row represents results from one of the three allocation strategies. The growth rate is defined as the relative density change of cells during the log phase [35]. The unit for time is days.

dashed lines in figure 2*f*). A similar effect is observed when the $+/+$ cell frequency is below the stable state value (see the green dotted lines in figure 2*f*) as long as the $f_+(0)$ is higher than the value $f_+^{us} = 0.069$ corresponding to the internal unstable state. Therefore, the two types of cells coexist, leading to a stable heterogeneous state. We also observe that producers would be extinct (see the blue dash-dotted line in figure 2*f*) if a small amount of $+/+$ cells are mixed with a large population of $-/-$ cells initially. These findings based on the replicator equations with nonlinear w_- are consistent with the experimental observations obtained in the presence of a small amount of exogenous resources [35].

3.3. Role of the exogenous production of public goods

From equation (3.5), it is clear that the stable state could also be influenced by extrinsic factors, such as the supply of exogenous resources. By varying the values of the parameter c_0 in equations (3.5) and (3.7), we investigated the role of exogenous resources in public goods game. The growth rate of the two different types of cells as a function of the fraction of $+/+$ cells is shown in figure 3 as the supply of exogenous resources (serum in the experiments [35] containing IGF-II molecules) is changed.

Figure 3*a* shows that $-/-$ cells grow faster than $+/+$ cells irrespective of the fraction f_+ of $+/+$ cells given large enough exogenous public goods (large c_0). Surprisingly, we find that the non-producer would sweep through the population while the producer becomes extinct (see the filled blue circle in figure 3*a*) even though the latter could get additional public goods produced by themselves ($b/a \ll 1$). This is due to the competitive advantage of the non-producers in a high welfare environment without punishment. These two cell types compete but do not cooperate with each other in nutrient-abundant environments.

As we decrease the serum concentration (smaller c_0) and keep all other parameters the same as in figure 3*a*, the two cell types start to establish a cooperative relationship and could coexist (figure 3*b*). This leads to the appearance of a stable heterogeneous state (see the filled green circle in figure 3*b*), indicating that cooperation could be established more

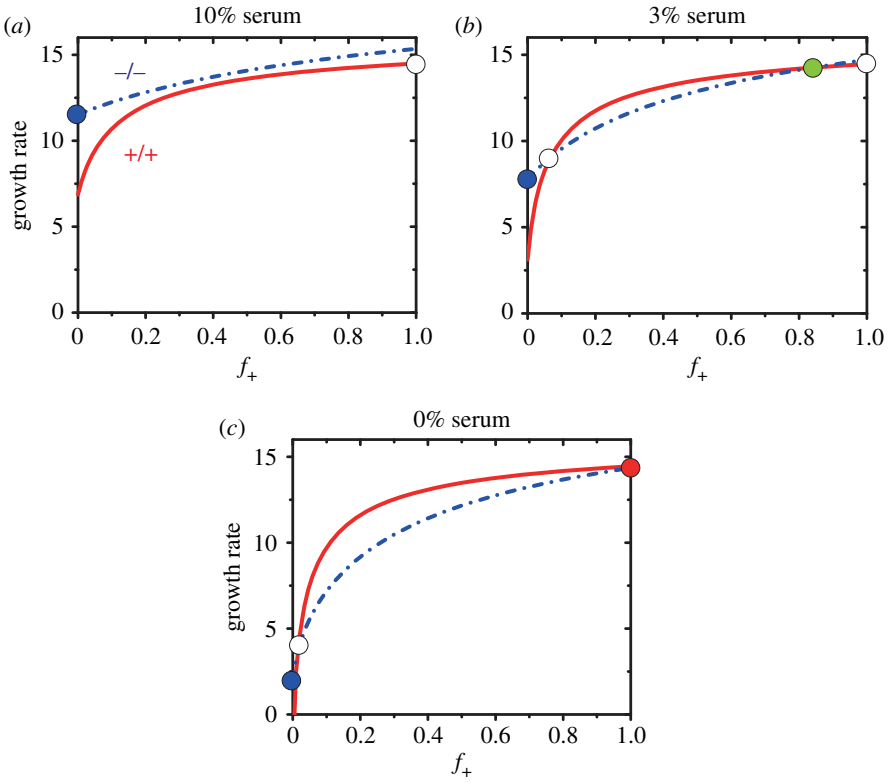

Figure 3. Growth rates of $+/+$ and $-/-$ cells as a function of the fraction (f_+) of $+/+$ cells at different levels of exogenous resources (serum). (*a*) $c_0 = 3.3$ corresponds to 10% serum in experiments; (*b*) $c_0 = 1$ represents 3% serum; (*c*) $c_0 = 0$ implies the absence of serum. The value of $a = 80$, $b = 8$ and $p_0 = 4.65$, corresponding to the parameters in figure 2*c*. The flow diagram in figure 3*b* corresponds to figure 2*c*. The meaning of the symbols used and the definition of growth rate are the same as in figure 2.

readily under harsh conditions (small available exogenous resources). In addition, the whole system could attain higher fitness or drug resistance (see more detailed discussions later) due to the coexistence of both the players. It is well known that many cancer cells have to confront hypoxia, low pH, low glucose and other severe conditions [53,54], and they are often found to be more aggressive and dangerous compared to cancer cells under normal growth conditions with access to essential nutrients [55]. These conditions might make it favourable to establish cooperation among them, leading to the formation of heterogeneous populations.

If exogenous resources removed from the system completely ($c_0 = 0$), the $+/+$ cells dominate the whole population while the $-/-$ cells would be swept away (see the red filled circle in figure 3*c*) at sufficiently high $f_+(0)$. In the opposite limit ($f_+(0)$ is small), the $-/-$ cells can take over the whole population (see the blue filled circle in figure 3*c*). The phenomenon of tragedy of the commons will be observed if the public goods are essential for the survival of non-producers. Taken together, these results show that the establishment of cooperation between different players shows strong dependence on environmental conditions. The influences of exogenous public goods as observed in figure 3 are consistent with the experimental results [35], and are further discussed below.

3.4. Comparison with *in vitro* experiments

Based on the calculations presented so far, we can now obtain the internal equilibrium fractions (f_+^i) of $+/+$ cells at different concentrations of serum. The experimental observations for f_+^i are given by symbols in figure 4*a*. The fractions f_+^s (f_+^{us}) under a stable (unstable) internal state are represented by red squares (blue circles). From the experimental result (figure 1*a*) in [35] for the equal fitness (≈14.4) of producer and non-producer cells and the fraction of $+/+$ cells approaching 1 for the stable internal state at $c_0 = 0$, we obtain the parameter $b \approx 8$. Our theoretical model with two free parameters a and p_0 fits the experimental results very well (see the solid red and blue lines in figure 4*a*). One scale parameter has been used with $c_0 = 1, 2, \ldots$ corresponding to 3%, 6%, … of serum.

To illustrate the stability of the internal equilibrium state, an example is given in figure 4*b*, which describes the evolution of the fraction of $+/+$ cells under different initial conditions ($f_+(0)$). The serum amount is fixed at 3%. It shows clearly that a stable equilibrium state is attained as long as $f_+(0)$ is above f_+^{us}, corresponding to the unstable internal equilibrium state. Then, the two types of cells cooperate leading to coexistence. However, the $+/+$ cells could be swept out and only $-/-$ cells exist if $f_+(0)$ is below f_+^{us} (see the dotted line in the inset of figure 4*b*). From the results in figure 4*a*, it follows that there exists a critical concentration c_0^c for exogenous resources (around 7% of serum in the experiment [35]). A bistable system can be reached only if the concentration of serum is lower than c_0^c. One stable state corresponds to a heterogeneous system with two subpopulations and the other one is a homogeneous state consisting of only $-/-$ cells (figure 3*b*). In this scenario, maintenance of heterogeneous state is due to cooperation between $+/+$ and $-/-$ cells. By contrast, as the concentration of serum increases beyond c_0^c, the $-/-$ cells can always obtain sufficient resources to support a faster growth rate than $+/+$ cells (figure 3*a*). Then, the $-/-$ cell would sweep through the whole population as long as its initial fraction is non-zero. Therefore, competition rather than cooperation is promoted between cell subpopulations under

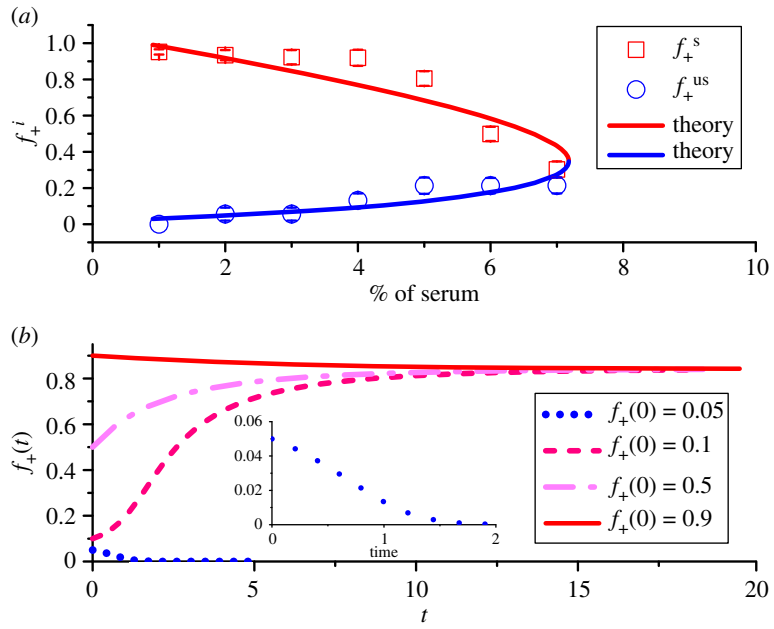

Figure 4. (*a*) The internal equilibrium fractions (f_+^i, $i \equiv s$ or us, with *s* for stable and us for unstable state) of $+/+$ cells as a function of serum levels. Stable states are shown by red squares while blue circles indicate unstable states. The upper and lower bounds represent the upper and lower boundaries for the equilibrium fractions observed in experiments and the symbols give the middle value of these two boundaries. The solid lines correspond to theoretical predictions using $a = 80$, and $p_0 = 4.65$ in equations (3.6) and (3.7). (*b*) Theoretical predictions for the time-dependent changes in the fraction $f_+(t)$ of $+/+$ cells for various initial conditions ($f_+(0)$=0.05, 0.1, 0.5, 0.9) in the presence of 3% of serum. The inset figure shows the evolution of the fraction of $+/+$ cells with $f_+(0) = 0.05$. The unit for time is days.

resource-abundant conditions. It eventually leads to the establishment of a homogeneous system with only a single type of cell population.

3.5. Effects of price paid by producers

In previous sections, we established that supply and allocation of public goods play crucial roles in determining the interactions among subpopulations. We investigate the influence of another parameter p_0, the price paid by $+/+$ cells to produce the public goods, which in the AFC experiment is IGF-II. The fitness of producers is affected by this parameter directly (see equation (3.6)), so we anticipate that it will influence the relationship between producers and non-producers.

Just as in figure 4, we investigated the internal equilibrium fraction f_+^i of producers as a function of the level of exogenous resources but differing values of p_0. The stable internal equilibrium fraction of producers is represented by the red curves, while the blue curves report the unstable internal equilibrium fraction (figure 5*a*). A critical p_0-dependent concentration for exogenous resources is observed in figure 4 above which non-producers can maintain a stable homogeneous system irrespective of the fate of the producers. The value of the critical concentration (see the red arrows in figure 5*a*) increases as p_0 decreases. The fitness of producers increases as they pay a much lower price (smaller p_0) for public goods production. Therefore, additional exogenous resources have to be provided to enhance the competitive advantage of non-producers at small p_0. We also observed another critical value (indicated by the star symbols in figure 5*a*) for exogenous resources at relatively small p_0 values. Only stable homogeneous states (consisting of either producers or non-producers) exist if the level of exogenous resources falls below this critical value. Interestingly, it becomes easier for the producer to establish a stable homogeneous system as p_0 decreases. On the other hand, only a small increase of exogenous resources leads to a homogeneous tumour consisting of only non-producers, as p_0 takes on large values (see the dotted line in figure 5*a*).

From figure 5*a*, we obtain the phase diagram in terms of the variables of the exogenous public goods concentration, and the initial fraction $f_+(0)$ of producers. Two examples shown in figure 5*b*,*c* with $p_0 = 4.65$ and $p_0 = 4.0$, respectively, show the emergence of three stable phases. At low levels of exogenous resources and large $f_+(0)$, a homogeneous phase with only producers (shown in pink colour) exists. The second homogeneous phase, with only non-producers (shown in blue colour), is easily accessible at high levels of exogenous resources. A heterogeneous phase representing the coexistence of both producer and non-producer cells (purple colour) can be attained at intermediate levels of exogenous resources and large $f_+(0)$. By comparing figure 5*b*,*c*, we find that the parameter space for the non-producer to take over the whole system shrinks as p_0 decreases while it increases for the producer to dominate the system. These figures also show that a heterogeneous system might be established easily (within a larger parameter space, comparing the purple region in figure 5*b*,*c*) if the producer pays a relatively high price for public goods production. From these discussions, we conclude that the price p_0 paid by producers greatly influences the state of the tumour, especially the robustness of the heterogeneous state. It appears that one can design better treatment protocols for cancers composed of different subpopulations by regulation of certain parameters, such as p_0 discussed here.

3.6. Cooperation among cancer subpopulations in *in vivo* experiments on glioblastoma

The mechanism of cooperation and feedback described through the replicator equations might be operative in other

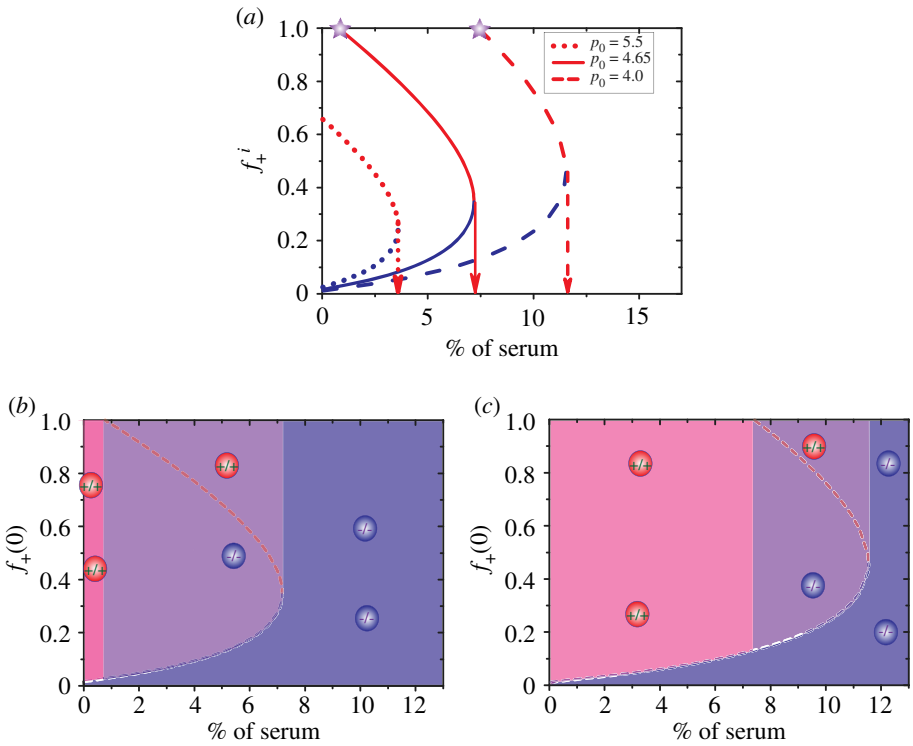

Figure 5. (a) The internal equilibrium fractions (f_+^i, $i \equiv s$, us) of producers as a function of the levels of serum for different p_0 values. The fraction (f_+^s) at stable equilibrium is shown in red colour while blue colour indicates unstable equilibrium fractions (f_+^{us}). Arrows give the critical level of serum above which only non-producers exist. Purple stars represent the lowest level of serum at which producers and non-producers coexist in a stable equilibrium state. (*b*,*c*) Phase diagrams (initial fraction $f_+(0)$ versus % of serum) with $p_0 = 4.65$ and $p_0 = 4.00$, respectively. Three stable phases are shown in these two figures. (i) A homogeneous phase consisting of only producers (pink colour). (ii) A heterogeneous phase consisting of both producers and non-producers (purple colour). The stable equilibrium fraction of producers is indicated by the dashed red line. (iii) A homogeneous phase with of only non-producers (blue colour). The red and blue circles represent the producer and non-producer cells, respectively. Remarkably, for both p_0 values $+/+$ and $-/-$ cells coexist in a narrow range of % of serum.

cancers. In order to illustrate the applicability of our theory, we analyse the origin of ITH in GBM. It is known that GBM is the most common and aggressive primary brain cancer with poor prognosis. The 5-year survival rate is less than 5%, and most patients live for only a year following diagnosis and treatment [56]. The extensive presence of ITH in GBM is well known at the genetic, molecular and cellular levels [57,58]. As in many other types of cancers, the mechanism for the origin of heterogeneity in GBM remains unclear, which is one reason for the poor design of effective treatment.

It is established [59–61] that chromosomal amplification of epidermal growth factor receptor gene (EGFR) is present in most cells of many primary GBMs. Another type of cell, showing intragenic rearrangement of EGFR gene (with deletion of exons 2–7) also frequently appear in the same tumour [62]. The coexistence of these two types of cells with differing expressions of the growth factor receptor leads to a worse prognosis of GBM [63,64] than would be the case when the cell (with EGFR gene rearrangement) is absent.

Recently, an experiment [34] studied the interactions between tumour cells with amplified levels of EGFR (referred to wt cells) and cells with rearrangement of EGFR gene (called Δ cells) within a neoplasm. It is found that the total size of the tumours (after 12 days of orthotopic injection) is much larger if a mixture of wt and Δ cells are injected into one mouse simultaneously than when they are injected into two mice separately. This finding shows that these two types of cells cooperate with each other to promote growth of the tumour. The producer (Δ) cells secrete certain factors like interleukin-6 (IL-6) and/or leukaemia inhibitory factor (LIF), which enhance the proliferation and inhibit apoptosis of tumour cells [34,65]. The system composed of wt and Δ cells is analogous to the one considered in the previous sections with IL-6 and/or LIF playing the role of the public goods. Therefore, we can apply our theory to investigate the consequence of cooperation between these two cell types in GBM.

In the experiment [34], the evolution of tumour size was measured over a wide range of conditions. A fixed total number of tumour cells (with differing fractions of wt and Δ cells) was injected into nude mice, and then the increase in the tumour volume was measured after different periods of time (see the inset in figure 6). Without Δ cells, it is difficult for the wt cells to induce tumour formation in nude mice, as illustrated by the pink upside-down triangles. However, the Δ cell alone gives rise to tumours at a rapid growth rate, as illustrated by the blue squares in figure 6. As long as a small fraction of Δ cells is injected into the mice together with wt cells, fast-growing tumours are induced in mice (see the purple up-triangles in figure 6). The tumour grows faster as the fraction of Δ cells in the total injected cells increases from 0%, 10%, 50% to 90% as shown in the inset of figure 6. It is also remarkable that the tumours grow even faster as the injected cells are composed of 10% wt and 90% Δ cells (green spheres) than is the case when 100% of cells are Δ cells (blue squares), which again shows that cooperation between the two cell types leads to an enhanced growth rate.

The experimental observations [34] can be quantitatively explained by the theoretical model developed here. By using the three growth curves (0%, 50% and 100% Δ cells) for the

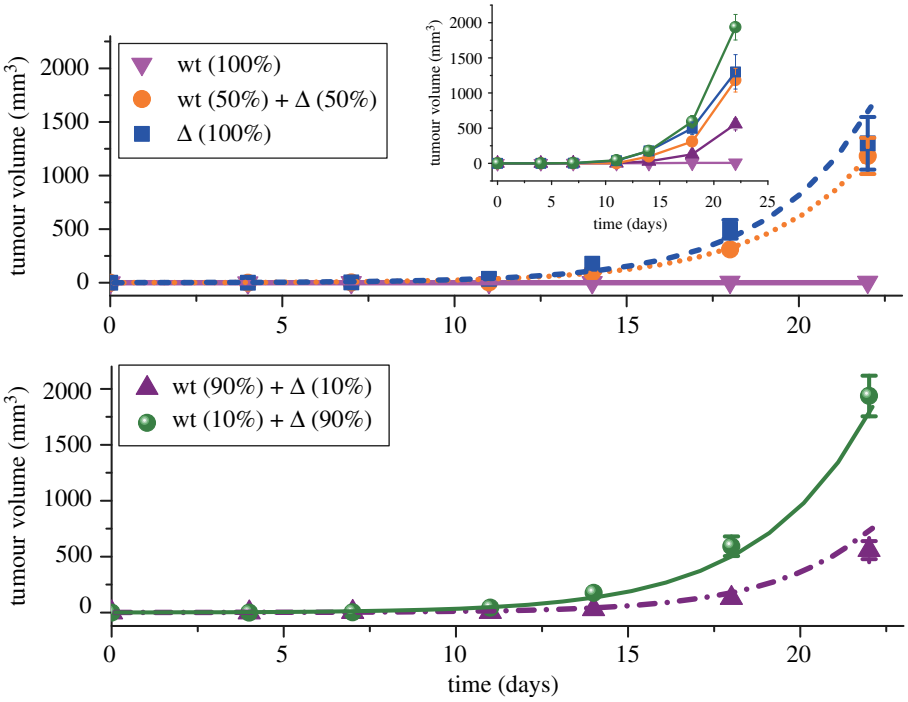

Figure 6. The evolution of tumour size as a function of time (in days) in glioblastoma with only wt cells, mutated Δ cells, or a mixture of these two types of cells (wt +Δ) injected into nude mice. The symbols represent experimental data. The parameter values ($a = 68.4$, $b = 0.946$ and $p_0 = 0.651$) in the model are obtained by fitting the theory to experimental data (details in the SI) with 100% wt, 100% Δ and 50% for each type of cells (upper panel). Lower panel: The purple and green curves are theoretical predictions with 10%, and 90% of Δ cells, which both agree quantitatively with experimental observations. Error bars represent the standard error of the mean in experiments. The complete experimental data are shown in the inset (the labels are the same as in the main figure).

tumours, illustrated in the upper panel of figure 6, we determined all the free parameters needed in the model (see the electronic supplementary material for details). Then, the evolution of the tumour size at differing conditions can be predicted. The theoretical predictions for the tumour growth at 10%, and 90% of Δ cells agree quantitatively with experimental observations, as shown in the lower panel of figure 6. To further explain the growth curves shown in the inset of figure 6, we plotted the growth rate of tumours as a function of the fraction of Δ cells (see the solid red line in figure 7). The growth rates for wt and Δ cells in the tumour are illustrated by dotted and dashed lines in figure 7, respectively. From this figure, it follows that the tumour growth rate increases as the fraction of Δ cells increases, reaching a maximum value in the middle (0.77, marked by the orange arrow). Subsequently, the rate starts to decrease. This behaviour is similar to the experimental data in the inset of figure 6 and is also found for pancreatic cancer cells, as discussed here and discovered by AFC [35].

We also found that the glioblastoma with ITH is quite stable irrespective of the initial composition (see electronic supplementary material, figure S5A). Our results explain the finding that frequently the wt cells and Δ cells coexist in GBM, and provides an explanation for the poor prognosis due to the quick recovery of the fast-growing state as long as a small fraction f_+ of Δ cells is present. Therefore, the stability of such a heterogeneous tumour needs to be eliminated in order to improve the survival rates of GBM patients. From the discussion above, it follows that the supply of exogenous pubic goods can influence cooperation between two different populations sharing one public good. By adding exogenous cytokines to the model (see electronic supplementary material, equations (S.7) and (S.8)), a stable homogeneous system composed of only wt cells could be

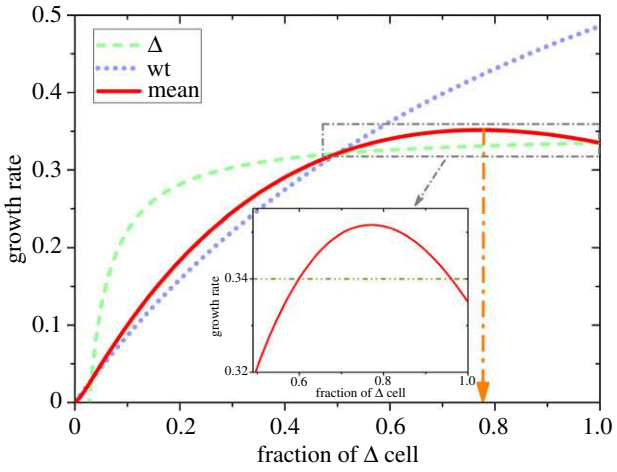

Figure 7. Predictions of the mean growth rate of the GBM tumour cells as a function of the fraction of the Δ cell. The green dashed line gives the growth rate of Δ cells, and the purple dotted line shows the rate of wt cells. The average growth rate of the whole population with both types of cells is given by the solid red line. A maximum is observed at a value $f_+ \approx 0.77$ (the orange arrow). The inset shows a zoom-in of the dash-dotted line rectangle. The values for the parameters a, b and p_0 in this figure are the same as the ones used in figure 6. The unit for growth rate is per day.

reached (see electronic supplementary material, figure S5B) irrespective of the initial fraction of the producer, Δ cells. Such a tumour would stop growing after removal of exogenous cytokines as wt cells alone cannot sustain tumour growth, as observed in experiments [34]. If practice, this might provide a treatment strategy for GBM, and perhaps other types of cancers dominated by ITH due to the interactions among different cancer cells.

4. Discussion

In this article, we investigated the interactions between two distinct subpopulations frequently observed in many cancers, which is a manifestation of heterogeneity. We uncovered a general mechanism for the establishment of a stable heterogeneous system consisting of producers and non-producer cells as a function of a number of experimentally controllable parameters. The tragedy of the commons would be expected as the public goods are shared equally among both the populations. However, a stable heterogeneous state arises if the producer can obtain the public goods more efficiently than the non-producer. Most importantly, the emergence of these scenarios require that the fitness of the two players must be a nonlinear function of the public goods. Otherwise, only an unstable heterogeneous system can be established. In addition, the cost-to-benefit ratio is a critical factor in determining the establishment of a stable coexisting state. In the experiments [35], the benefit is adjusted by changing the amount of serum while the cost of public good production is a constant. However, Archetti *et al.* changed the cost instead of benefit to study the cooperation and competition of the two types of cells in their model. This is due to the complex pay-off function assumed in the AFC model. In our model, the benefit of public goods is separated into two parts (endogenous and exogenous) naturally, while the cost is a constant. Therefore, we can investigate the influence of benefits on the cell cooperation and competition directly, as realized in experiments. In addition, our formulation is sufficiently general that we could test the effects of all other experimentally accessible parameters in order to assess the ranges of parameters that produce coexistence between producer and non-producer cells, as illustrated for the specific case in figure 5*b*.

We also found that it is relatively easy to establish cooperation and form a stable diversified or heterogeneous state in harsh conditions than in resource-abundant conditions. Such a phenomenon is quite common in biological systems [66,67]. The price paid by the producers also strongly influences the cooperation between the two players. A higher price can decrease the demand for exogenous resources in order to establish cooperation and might also expand cooperation to a wide parameter range.

Frequently in many cancers a minor subclone could support the growth of the whole tumour consisting of many different subpopulations [25–27]. It is easy to detect the genotype of dominant subclones, which would be considered as the target in later treatments. However, if a minor subclone escapes detection then it could survive, promoting a faster and more aggressive tumour growth caused by the competitive release [68]. Therefore, it is essential to learn the composition of a heterogeneous tumour, and also the interactions among different subclones before efficacious treatment can be formulated for the patients.

For cancers with producer and non-producer cells discussed here, it might be prudent to feed these cells instead of depriving them of nutrients so that competition between different subclones is promoted. Then, an effective treatment can be implemented as the system transits from a stable heterogeneous population to a homogeneous population. We have illustrated this concept using an experiment involving glioblastoma. This idea is reminiscent of another concept in cancer therapy, the tumour vasculature normalization [69]. The tumour vasculature is quite abnormal, which leads to heterogeneous tumour blood flow. Therefore, many tumour cells cannot get access to blood vessels and live under pressure such as hypoxia and acidosis, thus inducing genome instability and high intratumour heterogeneity [70]. Temporal normalization of tumour vasculature can reduce the microenvironment pressure on tumour cells and also increase the drug delivery efficiency. Hence, it can increase the conventional therapy efficacy if both procedures are scheduled carefully [69]. Similarly, the new idea proposed here could be combined with traditional therapies, such as surgery and chemotherapy, to reduce the risk and drug resistance but increase therapy efficacy. In addition, similar public goods dilemmas have been observed in many systems, such as microbial colonies, insect communities and human society [71–73]. The mechanism proposed here for the establishment of a heterogeneous population is quite general, and could in principle be applied to these systems. It will be most interesting to extend our model to the case beyond two species, which is more prevalent in nature [74]. It would be fruitful to consider different mechanisms of ITH in order to account for complex origins of ITH [12].

Data accessibility. The datasets supporting the article have been uploaded as part of the electronic supplementary material.

Authors' contributions. X.L. and D.T. conceived and designed the project, and co-wrote the paper. X.L. performed the research.

Competing interests. We declare we have no competing interests.

Funding. This work is supported by the National Science Foundation (PHY 17-08128 and CHE 16-32756) and the Collie-Welch Chair through the Welch Foundation (F-0019).

Acknowledgements. We are grateful to Marco Archetti, Abdul N. Malmi-Kakkada and Sumit Sinha for discussions and comments on the manuscript.

References

1. Gerlinger M, McGranahan N, Dewhurst SM, Burrell RA, Tomlinson I, Swanton C. 2014 Cancer: evolution within a lifetime. *Annu. Rev. Genet.* **48**, 215–236. (doi:10.1146/annurev-genet-120213-092314)
2. Nowell PC. 1976 The clonal evolution of tumor cell populations. *Science* **194**, 23–28. (doi:10.1126/science.959840)
3. Vogelstein B, Papadopoulos N, Velculescu VE, Zhou S, Diaz LA, Kinzler KW. 2013 Cancer genome landscapes. *Science* **339**, 1546–1558. (doi:10.1126/science.1235122)
4. Gerlinger M *et al.* 2012 Intratumor heterogeneity and branched evolution revealed by multiregion sequencing. *New Engl. J. Med.* **366**, 883–892. (doi:10.1056/NEJMoa1113205)
5. Sottoriva A, Spiteri I, Piccirillo SG, Touloumis A, Collins VP, Marioni JC, Curtis C, Watts C, Tavaré S. 2013 Intratumor heterogeneity in human glioblastoma reflects cancer evolutionary dynamics. *Proc. Natl Acad. Sci. USA* **110**, 4009–4014. (doi:10.1073/pnas.1219747110)
6. Bashashati A *et al.* 2013 Distinct evolutionary trajectories of primary high-grade serous ovarian cancers revealed through spatial mutational profiling. *J. Pathol.* **231**, 21–34. (doi:10.1002/path.4230)
7. Gerlinger M *et al.* 2014 Genomic architecture and evolution of clear cell renal cell carcinomas defined

by multiregion sequencing. *Nat. Genet.* **46**, 225–233. (doi:10.1038/ng.2891)

8. de Bruin EC *et al.* 2014 Spatial and temporal diversity in genomic instability processes defines lung cancer evolution. *Science* **346**, 251–256. (doi:10.1126/science.1253462)
9. Yates LR *et al.* 2015 Subclonal diversification of primary breast cancer revealed by multiregion sequencing. *Nat. Med.* **21**, 751–759. (doi:10.1038/nm.3886)
10. Boutros PC *et al.* 2015 Spatial genomic heterogeneity within localized, multifocal prostate cancer. *Nat. Genet.* **47**, 736–745. (doi:10.1038/ng.3315)
11. Ling S *et al.* 2015 Extremely high genetic diversity in a single tumor points to prevalence of non-Darwinian cell evolution. *Proc. Natl Acad. Sci. USA* **112**, E6496–E6505. (doi:10.1073/pnas.1519556112)
12. Almendro V, Marusyk A, Polyak K. 2013 Cellular heterogeneity and molecular evolution in cancer. *Annu. Rev. Pathol. Mech. Dis.* **8**, 277–302. (doi:10.1146/annurev-pathol-020712-163923)
13. Bedard PL, Hansen AR, Ratain MJ, Siu LL. 2013 Tumour heterogeneity in the clinic. *Nature* **501**, 355–364. (doi:10.1038/nature12627)
14. Zhang J *et al.* 2014 Intratumor heterogeneity in localized lung adenocarcinomas delineated by multiregion sequencing. *Science* **346**, 256–259. (doi:10.1126/science.1256930)
15. Snuderl M *et al.* 2011 Mosaic amplification of multiple receptor tyrosine kinase genes in glioblastoma. *Cancer Cell* **20**, 810–817. (doi:10.1016/j.ccr.2011.11.005)
16. Szerlip NJ *et al.* 2012 Intratumoral heterogeneity of receptor tyrosine kinases EGFR and PDGFRA amplification in glioblastoma defines subpopulations with distinct growth factor response. *Proc. Natl Acad. Sci. USA* **109**, 3041–3046. (doi:10.1073/pnas.1114033109)
17. Liotta LA, Kohn EC. 2001 The microenvironment of the tumour–host interface. *Nature* **411**, 375–379. (doi:10.1038/35077241)
18. Allinen M *et al.* 2004 Molecular characterization of the tumor microenvironment in breast cancer. *Cancer Cell* **6**, 17–32. (doi:10.1016/j.ccr.2004.06.010)
19. Bhowmick NA, Neilson EG, Moses HL. 2004 Stromal fibroblasts in cancer initiation and progression. *Nature* **432**, 332–337. (doi:10.1038/nature03096)
20. Malmi-Kakkada AN, Li X, Samanta HS, Sinha S, Thirumalai D. 2018 Cell growth rate dictates the onset of glass to fluid-like transition and long time super-diffusion in an evolving cell colony. *Phys. Rev. X* **8**, 021025. (doi:10.1103/PhysRevX.8.021025)
21. Cleary AS, Leonard TL, Gestl SA, Gunther EJ. 2014 Tumour cell heterogeneity maintained by cooperating subclones in Wnt-driven mammary cancers. *Nature* **508**, 113–117. (doi:10.1038/nature13187)
22. Marusyk A, Tabassum DP, Altrock PM, Almendro V, Michor F, Polyak K. 2014 Non-cell-autonomous driving of tumour growth supports sub-clonal heterogeneity. *Nature* **514**, 54–58. (doi:10.1038/nature13556)
23. Chapman A, del Ama LF, Ferguson J, Kamarashev J, Wellbrock C, Hurlstone A. 2014 Heterogeneous tumor subpopulations cooperate to drive invasion. *Cell reports* **8**, 688–695. (doi:10.1016/j.celrep.2014.06.045)
24. Aceto N *et al.* 2014 Circulating tumor cell clusters are oligoclonal precursors of breast cancer metastasis. *Cell* **158**, 1110–1122. (doi:10.1016/j.cell.2014.07.013)
25. Mullighan CG, Phillips LA, Su X, Ma J, Miller CB, Shurtleff SA, Downing JR. 2008 Genomic analysis of the clonal origins of relapsed acute lymphoblastic leukemia. *Science* **322**, 1377–1380. (doi:10.1126/science.1164266)
26. Johnson BE *et al.* 2014 Mutational analysis reveals the origin and therapy-driven evolution of recurrent glioma. *Science* **343**, 189–193. (doi:10.1126/science.1239947)
27. Morrissy AS *et al.* 2016 Divergent clonal selection dominates medulloblastoma at recurrence. *Nature* **529**, 351–357. (doi:10.1038/nature16478)
28. Boucher DH, James S, Keeler KH. 1982 The ecology of mutualism. *Annu. Rev. Ecol. Syst.* **13**, 315–347. (doi:10.1146/annurev.es.13.110182.001531)
29. Menon R, Korolev KS. 2015 Public good diffusion limits microbial mutualism. *Phys. Rev. Lett.* **114**, 168102. (doi:10.1103/PhysRevLett.114.168102)
30. Zhou X *et al.* 2018 Circuit design features of a stable two-cell system. *Cell* **172**, 744–757. (doi:10.1016/j.cell.2018.01.015)
31. Wang RW, Sun BF, Zheng Q, Shi L, Zhu L. 2011 Asymmetric interaction and indeterminate fitness correlation between cooperative partners in the fig–fig wasp mutualism. *J. R. Soc. Interface* **8**, 1487–1496. (doi:10.1098/rsif.2011.0063)
32. Axelrod R, Axelrod DE, Pienta KJ. 2006 Evolution of cooperation among tumor cells. *Proc. Natl Acad. Sci. USA* **103**, 13 474–13 479. (doi:10.1073/pnas.0606053103)
33. Merlo LM, Pepper JW, Reid BJ, Maley CC. 2006 Cancer as an evolutionary and ecological process. *Nat. Rev. Cancer* **6**, 924–935. (doi:10.1038/nrc2013)
34. Maria-del Mar I *et al.* 2010 Tumor heterogeneity is an active process maintained by a mutant EGFR-induced cytokine circuit in glioblastoma. *Genes Dev.* **24**, 1731–1745. (doi:10.1101/gad.1890510)
35. Archetti M, Ferraro DA, Christofori G. 2015 Heterogeneity for IGF-II production maintained by public goods dynamics in neuroendocrine pancreatic cancer. *Proc. Natl Acad. Sci. USA* **112**, 1833–1838. (doi:10.1073/pnas.1414653112)
36. Hofbauer J, Sigmund K. 1998 *Evolutionary games and population dynamics*. Cambridge, UK: Cambridge University Press.
37. Hauert C, Holmes M, Doebeli M. 2006 Evolutionary games and population dynamics: maintenance of cooperation in public goods games. *Proc. R. Soc. B* **273**, 2565–2570. (doi:10.1098/rspb.2006.3600)
38. Nowak MA. 2006 Five rules for the evolution of cooperation. *Science* **314**, 1560–1563. (doi:10.1126/science.1133755)
39. Allen B, Gore J, Nowak MA. 2013 Spatial dilemmas of diffusible public goods. *Elife* **2**, e01169. (doi:10.7554/eLife.01169)
40. Nanda M, Durrett R. 2017 Spatial evolutionary games with weak selection. *Proc. Natl Acad. Sci. USA* **114**, 6046–6051. (doi:10.1073/pnas.1620852114)
41. Bauer M, Frey E. 2018 Multiple scales in metapopulations of public goods producers. *Phys. Rev. E* **97**, 042307. (doi:10.1103/PhysRevE.97.042307)
42. Blythe RA, McKane AJ. 2007 Stochastic models of evolution in genetics, ecology and linguistics. *J. Stat. Mech: Theory Exp.* **2007**, P07018. (doi:10.1088/1742-5468/2007/07/P07018)
43. Melbinger A, Cremer J, Frey E. 2010 Evolutionary game theory in growing populations. *Phys. Rev. Lett.* **105**, 178101. (doi:10.1103/PhysRevLett.105.178101)
44. Hardin G. 1968 The tragedy of the commons. *Science* **162**, 1243–1248. (doi:10.1126/science.162.3859.1243)
45. Chesson P. 2000 Mechanisms of maintenance of species diversity. *Annu. Rev. Ecol. Syst.* **31**, 343–366. (doi:10.1146/annurev.ecolsys.31.1.343)
46. Hauert C, Michor F, Nowak MA, Doebeli M. 2006 Synergy and discounting of cooperation in social dilemmas. *J. Theor. Biol.* **239**, 195–202. (doi:10.1016/j.jtbi.2005.08.040)
47. Archetti M. 2013 Dynamics of growth factor production in monolayers of cancer cells and evolution of resistance to anticancer therapies. *Evol. Appl.* **6**, 1146–1159. (doi:10.1111/eva.12092)
48. Kimmel GJ, Gerlee P, Brown JS, Altrock PM. 2018 Neighborhood size-effects in nonlinear public goods games. *bioRxiv*. p. 347401. (doi:10.1101/347401).
49. Christofori G, Naik P, Hanahan D. 1994 A second signal supplied by insulin-like growth factor II in oncogene-induced tumorigenesis. *Nature* **369**, 414–418. (doi:10.1038/369414a0)
50. Pollak M. 2008 Insulin and insulin-like growth factor signalling in neoplasia. *Nat. Rev. Cancer* **8**, 915–928. (doi:10.1038/nrc2536)
51. Gerlee P, Altrock PM. 2015 Complexity and stability in growing cancer cell populations. *Proc. Natl Acad. Sci. USA* **112**, E2742–E2743. (doi:10.1073/pnas.1505115112)
52. Ayala FJ, Campbell CA. 1974 Frequency-dependent selection. *Annu. Rev. Ecol. Syst.* **5**, 115–138. (doi:10.1146/annurev.es.05.110174.000555)
53. Harris AL. 2002 Hypoxia—a key regulatory factor in tumour growth. *Nat. Rev. Cancer* **2**, 38–47. (doi:10.1038/nrc704)
54. Kato Y, Ozawa S, Miyamoto C, Maehata Y, Suzuki A, Maeda T, Baba Y. 2013 Acidic extracellular microenvironment and cancer. *Cancer Cell International* **13**, 89. (doi:10.1186/1475-2867-13-89)
55. Gupta GP, Massagué J. 2006 Cancer metastasis building a framework. *Cell* **127**, 679–695. (doi:10.1016/j.cell.2006.11.001)
56. Gallego O. 2015 Nonsurgical treatment of recurrent glioblastoma. *Curr. Oncol.* **22**, e273–281. (doi:10.3747/co.22.2436)
57. Jung V, Romeike BF, Henn W, Feiden W, Moringlane JR, Zang KD, Urbschat S. 1999 Evidence of focal genetic microheterogeneity in glioblastoma multiforme by area-specific CGH on microdissected tumor cells.

J. Neuropathol. Exp. Neurol. **58**, 993–999. (doi:10.1097/00005072-199909000-00009)

58. Bonavia R, Cavenee WK, Furnari FB. 2011 Heterogeneity maintenance in glioblastoma: a social network. *Cancer Res.* **71**, 4055–4060. (doi:10.1158/0008-5472.CAN-11-0153)
59. Hurt MR, Moossy J, Donovan-Peluso M, Locker J. 1992 Amplification of epidermal growth factor receptor gene in gliomas: histopathology and prognosis. *J. Neuropathol. Exp. Neurol.* **51**, 84–90. (doi:10.1097/00005072-199201000-00010)
60. Jaros E, Perry R, Adam L, Kelly P, Crawford P, Kalbag R, Mendelow AD, Sengupta RP, Pearson AD. 1992 Prognostic implications of p53 protein, epidermal growth factor receptor, and Ki-67 labelling in brain tumours. *Br. J. Cancer* **66**, 373–385. (doi:10.1038/bjc.1992.273)
61. Schlegel J, Merdes A, Stumm G, Albert FK, Forsting M, Hynes N, Kiessling M. 1994 Amplification of the epidermal-growth-factor-receptor gene correlates with different growth behaviour in human glioblastoma. *Int. J. Cancer* **56**, 72–77. (doi:10.1002/ijc.2910560114)
62. Nishikawa R, Ji XD, Harmon RC, Lazar CS, Gill GN, Cavenee WK, Huang HJ. 1994 A mutant epidermal growth factor receptor common in human glioma confers enhanced tumorigenicity. *Proc. Natl Acad. Sci. USA* **91**, 7727–7731. (doi:10.1073/pnas.91.16.7727)
63. Shinojima N *et al.* 2003 Prognostic value of epidermal growth factor receptor in patients with glioblastoma multiforme. *Cancer Res.* **63**, 6962–6970.
64. Heimberger AB, Hlatky R, Suki D, Yang D, Weinberg J, Gilbert M, Sawaya R, Aldape K. 2005 Prognostic effect of epidermal growth factor receptor and EGFRvIII in glioblastoma multiforme patients. *Clin. Cancer Res.* **11**, 1462–1466. (doi:10.1158/1078-0432.CCR-04-1737)
65. Heinrich PC, Behrmann I, Serge H, Hermanns HM, M"uller-Newen G, Schaper F. 2003 Principles of interleukin (IL)-6-type cytokine signalling and its regulation. *Biochem. J.* **374**, 1–20. (doi:10.1042/BJ20030407)
66. Korolev KS, Xavier JB, Gore J. 2014 Turning ecology and evolution against cancer. *Nat. Rev. Cancer* **14**, 371–380. (doi:10.1038/nrc3712)
67. Hoek TA, Axelrod K, Biancalani T, Yurtsev EA, Liu J, Gore J. 2016 Resource availability modulates the cooperative and competitive nature of a microbial cross-feeding mutualism. *PLoS Biol.* **14**, e1002540. (doi:10.1371/journal.pbio.1002540)
68. Greaves M, Maley CC. 2012 Clonal evolution in cancer. *Nature* **481**, 306–313. (doi:10.1038/nature10762)
69. Jain RK. 2005 Normalization of tumor vasculature: an emerging concept in antiangiogenic therapy. *Science* **307**, 58–62. (doi:10.1126/science.1104819)
70. Bristow RG, Hill RP. 2008 Hypoxia and metabolism: hypoxia, DNA repair and genetic instability. *Nat. Rev. Cancer* **8**, 180–192. (doi:10.1038/nrc2344)
71. Dobata S, Tsuji K. 2013 Public goods dilemma in asexual ant societies. *Proc. Natl Acad. Sci. USA* **110**, 1656–1660. (doi:10.1073/pnas.1309010110)
72. Drescher K, Nadell CD, Stone HA, Wingreen NS, Bassler BL. 2014 Solutions to the public goods dilemma in bacterial biofilms. *Curr. Biol.* **24**, 50–55. (doi:10.1016/j.cub.2013.10.030)
73. Kaul I, Grungberg I, Stern MA. 1999 *Global public goods: international cooperation in the 21st century*. New York, NY: Oxford University Press.
74. Levine JM, Bascompte J, Adler PB, Allesina S. 2017 Beyond pairwise mechanisms of species coexistence in complex communities. *Nature* **546**, 56–64. (doi:10.1038/nature22898)